Assessment of the Electromagnetic Disturbance of a Glass Fiber Reinforced Composite Fencing Structure

Domenico Asprone, Ph.D.[1]; Dario Assante[2]; Andrea Chiariello, Ph.D.[3]; Gaetano Manfredi[4]; Giovanni Miano[5]; Andrea Prota[6]; and Guglielmo Rubinacci[7]

Abstract: This work addresses the assessment of the electromagnetic disturbance induced by a composite barrier—fencing airport structures—to radio-communication electromagnetic waves. The barrier is composed of glass fiber reinforced polymer (GFRP) tubular elements installed into a concrete base. Based on the electromagnetic properties of constituent materials, numerical analyses describing the electromagnetic phenomenon were carried out, simulating the barrier submerged into the electromagnetic field of interest. Furthermore, full-scale experimental tests were also performed on samples of the barrier in an anechoic chamber, reproducing the electromagnetic field generated by the radio-communication antennas. Both the numerical and experimental studies confirm that composites and, in particular, GFRPs result in low interference with electromagnetic fields. The main contribution to the interference is generated by the concrete base. However, it may be significantly reduced by using particular strategies, for example, in very high frequency omnidirectional range systems, by placing the concrete basement under the counterpoise level of the antennas.

DOI: 10.1061/(ASCE)CC.1943-5614.0000121

CE Database subject headings: Fiber reinforced polymer; Glass; Composite materials; Blasting; Fences; Case studies.

Author keywords: GFRP composites; Blast protection structures; Electromagnetic disturbance.

Introduction

It is widely accepted in the scientific community that fiber reinforced polymers (FRPs) present low electromagnetic disturbance. This feature is often referred to as one of the most significant advantages of using FRPs rather than steel in civil structures characterized by the presence of equipment generating electromagnetic fields [Mallick 1993; Chawla 1998; National Materials Advisory Board, National Academies Press (U.S.) 2005; Ryall 2001], e.g., radio-communication antennas in airport infrastructures or medical equipment in hospitals.

In 2007 AMRA, an Italian research center, led the Security of Airport Structures project, focusing on the design of a protection barrier, devoted to fence air traffic control sites. The structure was required to exhibit specific mechanical properties, to protect the fenced infrastructures from malicious disruptions, including blast terroristic attacks; moreover, the barrier was required to provide low disturbance to electromagnetic fields generated by antennas for air traffic control radio communications. Further requirements regarded low installation and maintenance costs and high durability.

In order to meet such requirements, a polymeric composite structure was considered. In particular, a discontinuous barrier was designed, consisting of glass fiber reinforced polymer (GFRP) tubular elements, vertically installed into a concrete base foundation. The constituent material is a pultruded polyester composite reinforced with unidirectional E-glass fibers; the volume fraction of fibers is about 60%. The designed fencing structure is depicted in the following figures: Fig. 1, where a prototype of the barrier is presented; a lateral view is also presented in Fig. 2, reporting the main dimensions of the structure. In particular, the concrete base was 0.5-m high, while the pipe elements were 2.5-m high, determining a total height of the barrier of 3 m. The interior distance between the pipes was 150 mm, while the total diameter of each element was 85 mm. The wall of the pipes was 5.5 mm thick, composed of an internal layer of 4.5 mm thick, with unidirectional fiber reinforcement, and two external layers of 0.5 mm thick with randomly distributed fiber reinforcement. GFRP was used also for the internal reinforcing rebar of the con-

[1]Dept. of Structural Engineering, Univ. of Naples "Federico II," via Claudio 21, 80125 Naples, Italy (corresponding author). E-mail: d.asprone@unina.it

[2]Assistant Professor, Faculty of Engineering, International Telematic Univ. Uninettuno, Rome, Italy.

[3]Dept. of Electrical Engineering, Univ. of Naples "Federico II," via Claudio 21, 80125 Naples, Italy.

[4]Full Professor, Dept. of Structural Engineering, Univ. of Naples "Federico II," via Claudio 21, 80125 Naples, Italy.

[5]Full Professor, Dept. of Electrical Engineering, Univ. of Naples "Federico II," via Claudio 21, 80125 Naples, Italy.

[6]Assistant Professor, Dept. of Structural Engineering, Univ. of Naples "Federico II," via Claudio 21, 80125 Naples, Italy.

[7]Full Professor, Dept. of Electrical Engineering, Univ. of Naples "Federico II," via Claudio 21, 80125 Naples, Italy.

Note. This manuscript was submitted on July 21, 2009; approved on March 16, 2010; published online on March 18, 2010. Discussion period open until March 1, 2011; separate discussions must be submitted for individual papers. This paper is part of the ***Journal of Composites for Construction***, Vol. 14, No. 5, October 1, 2010. ©ASCE, ISSN 1090-0268/2010/5-629–635/$25.00.

Fig. 1. Prototype of the barrier

crete base elements, in order to have a completely steel-free structure; a detail of the internal reinforcement configuration is presented in Fig. 3. The described configuration was chosen to guarantee that the barrier would deter malicious intrusions into protected sites; at the same time, it was expected that the structure could reduce the effects of a blast-induced overpressure on protected infrastructures caused by a malicious explosion event, by disrupting blast shock waves. Details about the behavior of the structure subjected to a blast-induced overpressure have been reported in Asprone et al. (2007), whereas the results of a mechanical characterization of the used GFRP under high dynamic loading conditions can be found in Asprone et al. (2009).

With regard to the electromagnetic requirements, the design was carried out considering the condition of the barrier placed close to a very high frequency omnidirectional range (VOR) antenna. VOR systems (Fig. 4) are composed of 36 antennas, circularly disposed on a metallic structure, communicating to flying aircraft their position with respect to the magnetic North. The antennas are posed over a metallic grid, providing a total reflection of the electromagnetic waves. The electromagnetic frequency range generated by VOR antennas varies between 100 MHz and 1 GHz and was considered to define the reference electromagnetic field passing through the barrier. The main objective of the analysis was to define how to place the barrier in proximity of the VOR, to avoid relevant disturbances to the system performances.

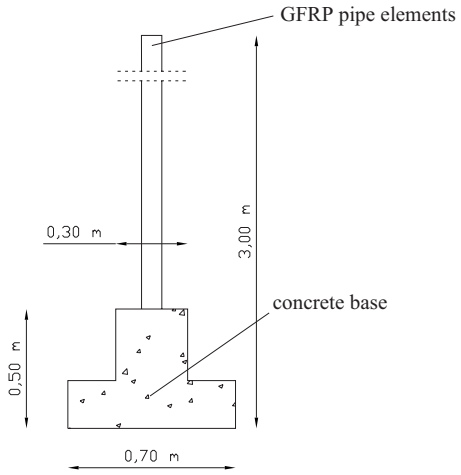

Fig. 2. Lateral view of the barrier

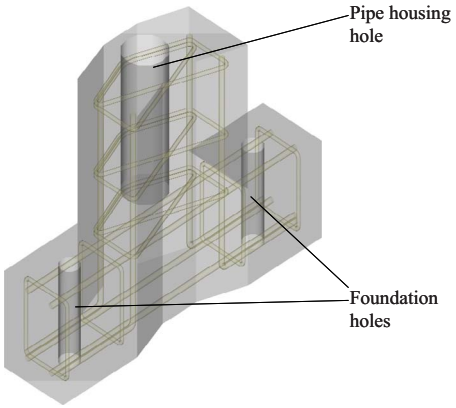

Fig. 3. Internal reinforcement of concrete base elements

In available literature a number of work focus on the electromagnetic propagation into commonly used construction materials, especially steel reinforced concrete, at radio frequencies typically used in civil environments (Pena et al. 2003; Richalot et al. 2000; Dalke et al. 2000; Savov and Herben 2003). However, no data appear available about the electromagnetic disturbance due to similar fencing structures, at the frequency of interest for this work.

Electromagnetic Characteristics of the Fencing System

The propagation of the electromagnetic field is described by the well-known Maxwell equations (Collin 1991). In these equations, the characteristics of the materials are taken into account in the constitutive relations between the different fields. Under the assumption of linear, homogeneous, isotropic, and nondispersive media, the relations between the fields appearing in the Maxwell equations are taken into account by three constants, namely, the relative dielectric permittivity ε_r, the relative magnetic permeability μ_r, and the electric conductivity σ. Different values of these three parameters lead to different electromagnetic behaviors of

Fig. 4. VOR station

the materials. The free space has a relative dielectric permittivity and a relative magnetic permeability equal to 1, while the electric conductivity is 0.

The barrier under examination is essentially constituted by GFRP and concrete. Both materials can be assumed linear, homogeneous, and reasonably isotropic in terms of electromagnetic parameters. In particular, the relative magnetic permeability of both these materials is almost 1 as they do not present magnetic properties.

The values of the relative dielectric permittivity of GFRP and concrete have been measured using the coaxial wire technique and are well known in literature. It is possible to assume a relative dielectric permittivity of about 3–4 for GFRP (Gallone et al. 2001) and 6–8 for concrete (Robert 1998), depending on the manufacturing, in a frequency range from 100 MHz to 1 GHz. The electric conductivity has also been measured and discussed in several papers in literature and it is about 3.5 μS/m for GFRP (Gallone et al. 2001; Casalini et al. 1997) and 0.01–0.1 S/m for concrete (Robert 1998; Soutsos et al. 2001). To evaluate how this property influences the behavior of the materials at a given frequency f, the quantities $2\pi f\sigma$ and $\varepsilon_0\varepsilon_r$ have to be compared (Collin 1991), where $\varepsilon_0 \approx 8.85 \times 10^{-12}$ F/m is the free-space dielectric permittivity. For the frequency of interest in our problem, the two terms are comparable for the concrete, while for GFRP $2\pi f\sigma$ is much smaller than $\varepsilon_0\varepsilon_r$. This means that the electric conductivity, for the frequencies of interest, has to be taken into account for the concrete and can be neglected for the GFRP.

Numerical Analysis

Preliminary Assessment

A simple but qualitatively significant result can be obtained considering the problem of the "dielectric slab," an infinite thick plane of a given material, characterized by a given relative dielectric permeability. Considering an incident plane wave, with arbitrary incident angle and polarization, on one side of the slab, it is possible to evaluate analytically the reflected and transmitted power of the plane wave on the sides of the slab and then to estimate the interference of the material as a function of the slab thickness (Collin 1991). This simple model is used only to give a quick preliminary evaluation of the interference introduced by the GFRP and concrete. Using for GFRP a typical range of thickness dimensions (5–15 mm) and frequency (100 MHz–1 GHz), in the worst case (thickness of 15 mm and frequency of 1 GHz) the transmitted power is 9.82% lower than the incident power. Instead if typical dimensions are used for concrete (10–50 cm), the transmitted power is reduced to the 10% of incident power. This suggests that the disturbance due to the GFRP poles is negligible and the main disturbance is due to the concrete basement.

Full-Wave 2D Analysis

In order to produce a more realistic model for the behavior of the fence in the presence of an electromagnetic field, a full-wave two-dimensional (2D) numerical analysis has been conducted using a finite-element tool (Dular et al. 1998). The geometry of the problem is shown in Fig. 5. A circular counterpoise, whose height and radius are 1 and 15 m, respectively, is posed over the ground plane, simulating the metallic grid at the basis of the VOR antennas; both the counterpoise and the ground are assumed to be electrically perfectly conductive. An electromagnetic source, represented as a loop of current, is placed 1 m above the counterpoise. Finally, a circular barrier is placed at the distance of 18 m from the center, composed of a concrete basement (ε_r=7, σ =0.01 S/m) and GRFP empty poles (ε_r=3). This model quite realistically reproduces the case of a VOR antenna, placed in the center of the counterpoise fenced by the developed structure. This assumption allows making qualitative evaluations with a reasonable computational effort, by means of the axial symmetry. The current loop well represents the Alford loop antenna usually adopted in the VOR stations, as it has the same horizontal polarization and a similar radiation pattern. To confirm this, in Fig. 6, the radiation pattern (half diagram, due to the axial symmetry) is shown for a typical Alford loop antenna (Milligan 2005) and for the considered structure without the fence. The typical dimension of the GFRP poles is small if compared to the wavelength, at typical VOR working frequency; then, from an electromagnetic point of view, they can be approximated by two cylindrical axial symmetric slabs separated by the diameter of the poles.

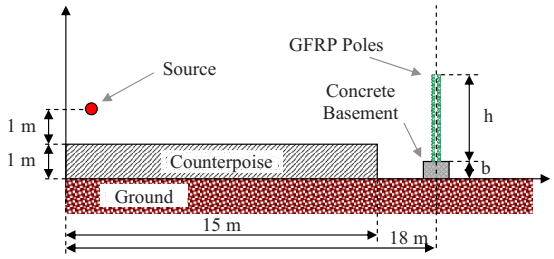

Fig. 5. Model for the numerical analysis

Actually, to study with particular accuracy the electromagnetic disturbance induced by the composite barrier on the actual VOR stations a three-dimensional numerical analysis is necessary, taking into account both the real shapes and the electromagnetic characteristics of the antenna, the counterpoise metallic grid, the GFRP poles, the concrete basement, and the surrounding environment. However, aiming to a qualitative assessment, the 2D axial symmetric analysis appears adequate.

The aim of this analysis is to evaluate the radiated power in the absence of the barrier or in the presence of a barrier, for different values of the height of the basement and of the poles; this can allow observing how the barrier affects the performance of the antenna. Case (a) is represented by a basement 0.5 m high and poles 2.5 m high (the basement is under the counterpoise level and tubes are over the counterpoise; this configuration is the most common for VOR sites, since the antennas are placed as

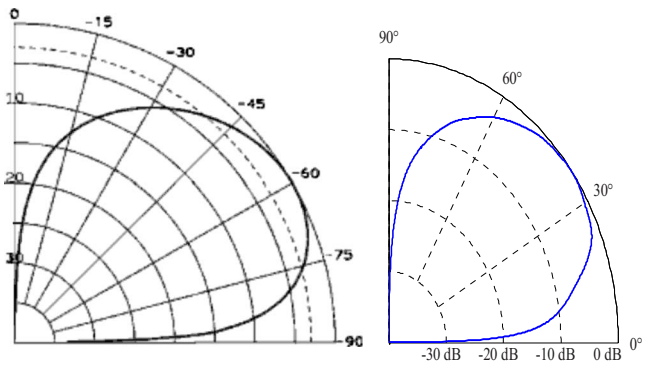

Fig. 6. Radiation pattern of an Alford loop antenna (left) and the considered structure (right)

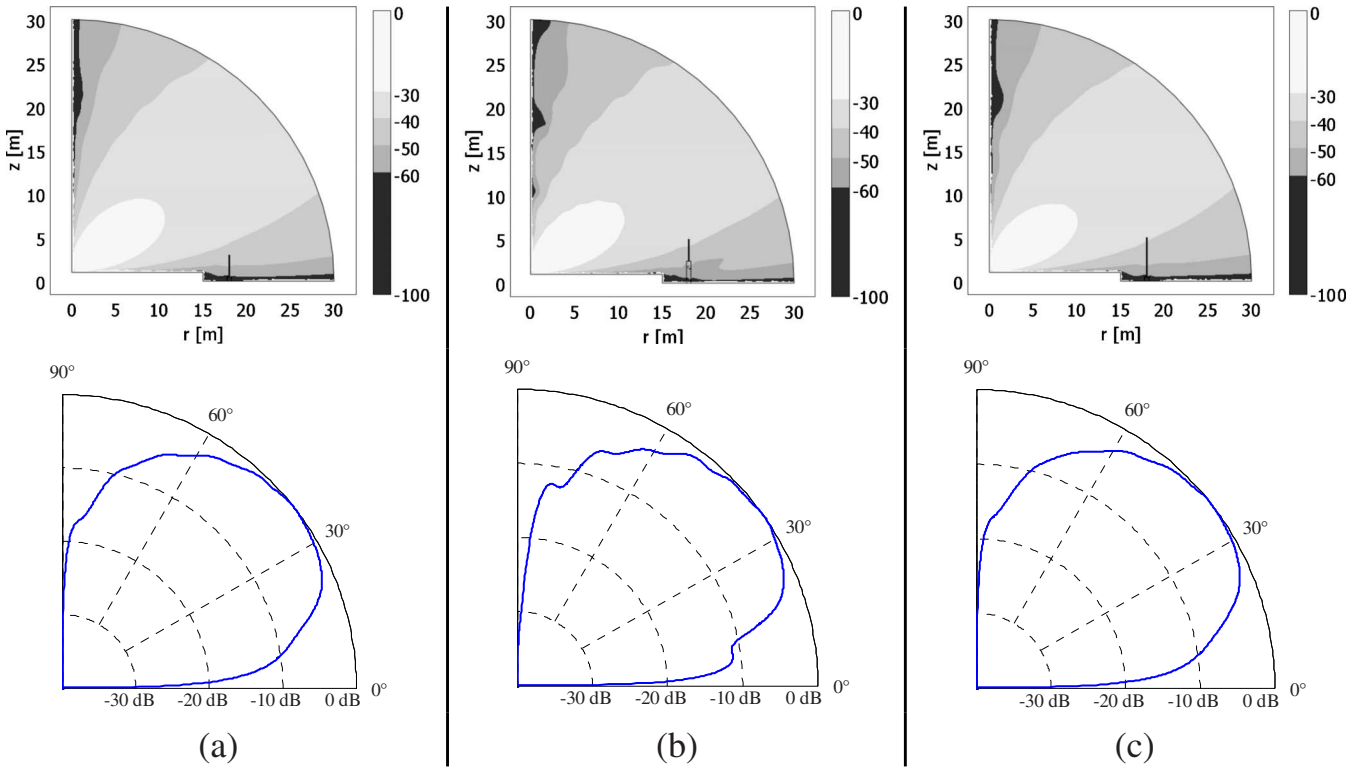

Fig. 7. Plot of the radiated power in dB and radiation patterns for Cases (a) (basement: 0.5 m, poles: 2.5 m), (b) (basement: 2.5 m, poles: 2.5 m), and (c) (basement: 0.5 m, poles: 4.5 m)

high as possible with respect to the ground). The radiation pattern of the whole system is depicted in Fig. 7(a) where a minimal variation occurs with respect to the unfenced case. Case (b) is represented by a basement 2.5 m high and poles 2.5 m high. Even if the basement usually does not reach this height, this case is relevant because it is representative of the situations where both the basement and the tubes are over the counterpoise level, as it could be due to orographic reasons. As it appears in Fig. 7(b), in this case, the radiation pattern has a valuable variation, due to the effect of the concrete over the counterpoise level. However, it could be supposed that the observed distortion of the radiation pattern is due to the presence of both the concrete basement and the GFRP poles. To clarify this aspect, Case (c) was also considered represented by a basement 0.5 m high and poles 4.5 m high (so that the total height of the structure is the same as in the previous case, but only the GFRP poles are over the counterpoise level). In this case, as shown in Fig. 7(c), a minimal distortion of the radiation pattern is observed; this proves that the main disturbance occurs when the concrete basement is over the counterpoise level. To quantify the disturbance, it is possible to evaluate a percentage error, which is defined as

$$E = \frac{\|P - P_0\|}{\|P_0\|} \times 100$$

where P=radiated power in the different cases and P_0=radiated power in the unfenced situation, as a function of the angle. The error has been evaluated for Cases (a)–(c) in the whole angular interval of 0°–90°; the results are shown in Table 1. The error E_{dB} has been also evaluated; it is defined similarly to the error E, but only in the 3-dB radiation angle (defined as the angular sector where the radiated power decreases less than 3 dB with respect to the maximum value); E_{dB} is mainly important for the behavior of the system. The results are shown in the same table. In both cases the determined values quantitatively confirm the previous considerations on the disturbances on the radiation pattern.

Once assessed that Cases (a) and (b) are the most significant, the attention has been focused on these cases, performing some parametric analyses. In Table 2 errors E and E_{dB} are computed for different values of the electric conductivity of the concrete, keeping the relative dielectric permittivity equal to 7. It is found that, as the electric conductivity increases, the error decreases if the basement is under the counterpoise and increases if the basement is over the counterpoise. This means that the previous suggestion

Table 1. Percentage Error of the Radiation Patterns for the Three Considered Cases

	E	$E_{3\ dB}$
Case (a)	1.68	1.30
Case (b)	5.56	4.07
Case (c)	1.71	1.42

Table 2. Percentage Error of the Radiation Patterns as a Function of the Electric Conductivity of the Concrete

	σ=0.01 S/m		σ=0.05 S/m		σ=0.1 S/m	
	E	$E_{3\ dB}$	E	$E_{3\ dB}$	E	$E_{3\ dB}$
Case (a)	1.68	1.30	1.17	0.85	1.16	0.84
Case (b)	5.56	4.07	6.20	4.77	6.99	5.47

Table 3. Percentage Error of the Radiation Patterns as a Function of the Dielectric Permittivity of the Concrete

	$\varepsilon_r=6$		$\varepsilon_r=7$		$\varepsilon_r=8$	
	E	$E_{3\ dB}$	E	$E_{3\ dB}$	E	$E_{3\ dB}$
Case (a)	1.57	1.24	1.68	1.30	1.70	1.30
Case (b)	5.55	4.28	5.56	4.07	5.67	3.91

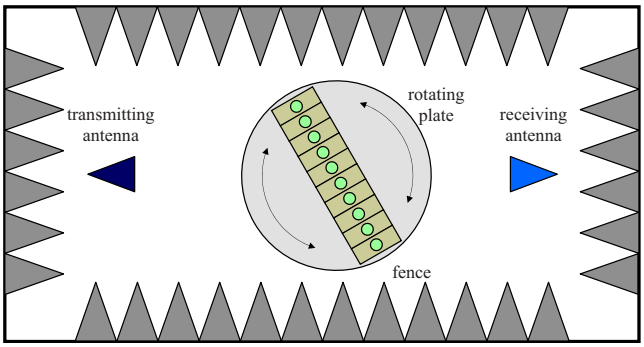

Fig. 8. Experimental setup

Fig. 9. Barrier and the transmitting antenna in the anechoic chamber

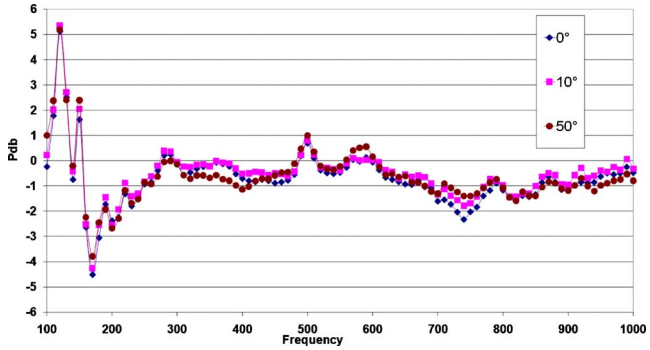

Fig. 10. Difference between the received powers (dB) with and without the barrier, for different angles (vertical polarization)

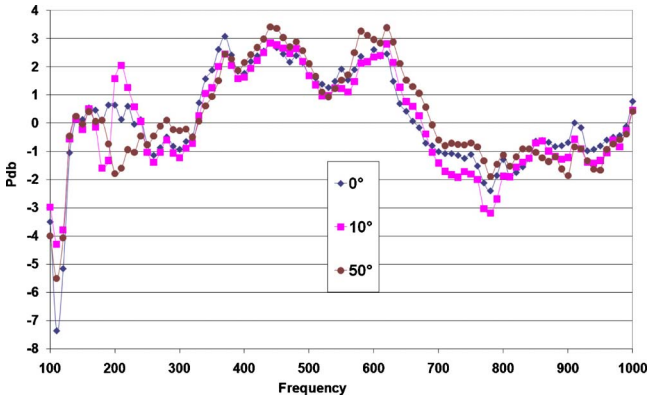

Fig. 11. Difference between the received powers (dB) with and without the barrier, for different angles (horizontal polarization)

to place the basement under the counterpoise level is much more important for higher values of the concrete electric conductivity, as expected.

Finally, in Table 3, the disturbance of the fence is analyzed for different values of the relative dielectric permittivity of the concrete, when the electric conductivity is equal to 0.01 S/m. In this case, it appears that the disturbance generally increases for higher values of relative dielectric permeability, as expected.

Experimental Program

Experimental analyses have been performed on a barrier prototype, composed of 19 tubes, for a total length of 3 m. The measurements have been performed in the anechoic chamber of the Department of Electrical Engineering of the University of Naples Federico II. The measurement scheme has been reported in Fig. 8: the barrier is placed in the middle of the chamber, over a rotating plate, between two antennas. The electromagnetic disturbance of the barrier is estimated by producing an electromagnetic wave with the transmitting antenna and evaluating the power drop at the receiving antenna. The anechoic chamber isolates the barrier and the antennas from external disturbances, and avoids interferences on the receiving antenna produced by reflections on the lateral walls by means of absorbing cones, reproducing the conditions of measurement in an open site.

The chamber is certified according to the standards EN 50147-2/ANSI C63.4, EN 61000-4-3, EN 50147-1, CISPR 16-1 up to a

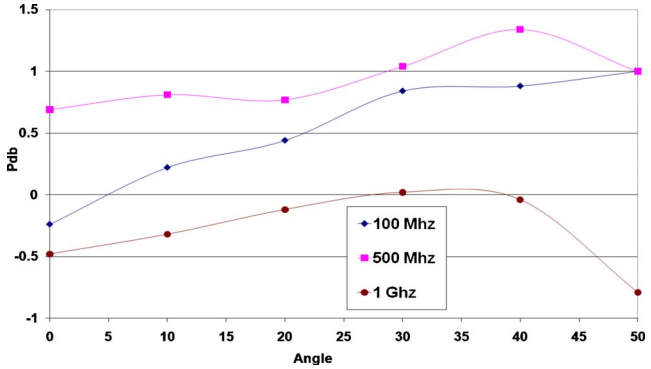

Fig. 12. Difference between the received powers (dB) with and without the barrier, for different frequencies (vertical polarization)

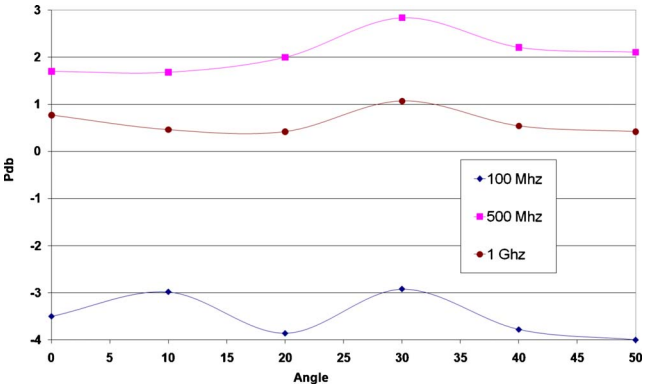

Fig. 13. Difference between the received powers (dB) with and without the barrier, for different frequencies (horizontal polarization)

frequency of 18 GHz. The chamber has a length of 9.05 m, a width of 5.85 m, and a height of 5.86 m. The certified quiet zone has a length of 4.15 m, a width of 2.80 m, and a height of 3.19 m. The antennas are both log periodic; an Amplifier Research AT1080A, operating in the frequency range 80–1,000 MHz as a transmitter, and a Schwarzbech VULB 9161, operating in the frequency range 30–1,600 MHz as a receiver, are placed at the opposite sides of the chamber. In Fig. 9, the barrier and the transmitting antenna are shown in the anechoic chamber. A Rohde and Schwarz SML03 signal generator and a Rohde and Schwarz Emi Test Receiver RF Analysis ESCS30 are employed for the measurement.

Defining PR and PR_0 as the received powers in the presence and absence of the barrier, for a given frequency of the incident radiation and position of the barrier, the quantity

$$P_{\mathrm{dB}} = 10 \log_{10} \frac{\mathrm{PR}}{\mathrm{PR}_0}$$

represents the difference between the received powers in the presence and absence of the barrier, expressed in decibels.

To evaluate the effect of the barrier on the propagation of the electromagnetic field, the polarization of the source field has to be taken into account as it can influence the result. The polarization is a property that describes the orientation of the oscillation of the electric field. The VOR antennas usually produce a linearly polarized electric field, that is, the direction is constant and is orthogonal to the propagation direction. In the following analyses both the cases of the electric field parallel (horizontal polarization) and orthogonal (vertical polarization) to the ground have been considered.

In Figs. 10 and 11, the difference between the received powers in the presence and absence of the barrier can be observed, for different values of the frequency. The figures refer to a vertically and a horizontally polarized electromagnetic field, respectively. In both cases, the measurements have been performed for different incidence angles, rotating the barrier with respect to the chamber and the antennas.

In Figs. 12 and 13, the same quantity is shown as a function of the incidence angle, for different frequencies, in case of vertical and horizontal polarizations. Considering that the accuracy of the measurement can be estimated as ± 5 dB, in all cases the effect of the barrier on the electromagnetic field appears very small. Significant differences between the power values measured in the presence and in the absence of the barrier are observed at lower frequencies, where the wavelength is comparable with the size of the anechoic chamber and a loss of accuracy occurs. In this case a more accurate analysis should be performed in an open test site. It is underlined that data scatter based on multiple tests is negligible for this application, since the wavelength (from 0.30 to 3.00 m) is much larger than the typical dimensions of the imperfections (about 1 mm) for the investigated elements. Hence significant variations in results are not expected.

Conclusions

The main objective of this work is to assess the low electromagnetic disturbance of composites and, in particular, of GFRP in a specific application. In particular, the electromagnetic behavior of an innovative GFRP barrier for air traffic control sites has been analyzed. Numerical and experimental researches have shown consistent results. The GRFP tubes seem to have a minimal influence on the electromagnetic field, whereas the concrete basement of the barrier has produced a more relevant disturbance, even if not reinforced with a steel rebar. In particular, the obtained data allow presuming that steel internal reinforcement would have not increased the disturbance introduced by the concrete elements. Hence, this study confirms the low electromagnetic disturbance of GFRP, which is reported in available literature as a characteristic of GFRP composites. On the contrary, with regard to the behavior of reinforced concrete, this study shows that concrete causes a significant electromagnetic disturbance for the investigated range of frequency, whereas the electromagnetic disturbance due to internal reinforcement appears negligible. Thus, the proposed barrier appears to fit the low disturbance requirements to fence air traffic control sites, if the concrete basement is placed under the counterpoise level of the antennas, which actually occurs in the most VOR sites.

References

Asprone, D., Cadoni, E., Prota, A., and Manfredi, G. (2009). "Strain-rate sensitivity of a pultruded e-glass/polyester composite." *J. Compos. Constr.*, 13, 558–564.

Asprone, D., Prota, A., Parretti, R., and Nanni, A. (2007). "Protection of airport facilities through radio frequency transparent fences: The SAS project." *CD-Proc., Performance, Protection and Strengthening of Structures Under Extreme Loading, PROTECT 2007*, Paper No. ITA02.

Casalini, R., Corezzi, S., Livi, A., Levita, G., and Rolla, P. A. (1997). "Dielectric parameters to monitor the crosslink of epoxy resins." *J. Appl. Polym. Sci.*, 65(1), 17–25.

Chawla, K. K. (1998). *Composite materials: Science and engineering*, Springer, New York.

Collin, R. E. (1991). *Field theory of guided waves*, IEEE, Piscataway, N.J.

Dalke, R. A., Holloway, C. L., McKenna, P., Johansson, M., and Ali, A. S. (2000). "Effects of reinforced concrete structures on RF communications." *IEEE Trans. Electromagn. Compat.*, 42(4), 486–496.

Dular, P., Geuzaine, C., Henrotte, F., and Legros, W. (1998). "A general environment for the treatment of discrete problems and its application to the finite element method." *IEEE Trans. Magn.*, 34(5), 3395–3398.

Gallone, G., Capaccioli, S., Levita, G., Rolla, P., and Corezzi, A. (2001). "Dielectric analysis of the linear polymerization of an epoxy resin." *Polym. Int.*, 50, 545–551.

Mallick, P. K. (1993). *Fiber-reinforced composites: Materials, manufacturing, and design*, CRC, Boca Raton, Fla.

Milligan, T. A. (2005). *Modern antenna design*, Wiley, New York.

National Materials Advisory Board, National Academies Press. (U.S.).

(2005). "Going to extremes: Meeting the emerging demand for durable polymer matrix composites." National Research Council (U.S.), 67.

Pena, D., Feick, R., Hristov, H. D., and Grote, W. (2003). "Measurement and modeling of propagation losses in brick and concrete walls for the 900-MHz band." *IEEE Trans. Antennas Propag.*, 51(1), 31–39.

Richalot, E., Bonilla, M., Wong, M. F., Fouad-Hanna, V., Baudrand, H., and Wiart, J. (2000). "Electromagnetic propagation into reinforced-concrete walls." *IEEE Trans. Microwave Theory Tech.*, 48(3), 357–366.

Robert, A. (1998). "Dielectric permittivity of concrete between 50 MHz and 1 GHz and GPR measurements for building materials evaluation." *J. Appl. Geophys.*, 40, 89–94.

Ryall, M. J. (2001). *Bridge management*, Butterworth-Heinemann, Stoneham, Mass.

Savov, S. V., and Herben, M. H. A. J. (2003). "Modal transmission-line modeling of propagation of plane radiowaves through multilayer periodic building structures." *IEEE Trans. Antennas Propag.*, 51(9), 2244–2251.

Soutsos, M. N., Bungey, J. H., Millard, S. G., Shaw, M. R., and Patterson, A. (2001). "Dielectric properties of concrete and their influence on radar testing." *NDT & E Int.*, 34, 419–425.